

Electronic structure of triangular, hexagonal and round graphene flakes near the Fermi level

H P Heiskanen, M Manninen, and J Akola

Nanoscience Center, Department of Physics, P.O.Box 35, FI-40014 University of Jyväskylä, Finland

E-mail: matti.manninen@jyu.fi

Abstract.

The electronic shell structure of triangular, hexagonal and round graphene quantum dots (flakes) near the Fermi level has been studied using a tight-binding method. The results show that close to the Fermi level the shell structure of a triangular flake is that of free *massless* particles, and that triangles with an armchair edge show an additional sequence of levels (“ghost states”). These levels result from the graphene band structure and the plane wave solution of the wave equation, and they are absent for triangles with a zigzag edge. All zigzag triangles exhibit a prominent edge state at ϵ_F , and few low-energy conduction electron states occur both in triangular and hexagonal flakes due to symmetry reasons. Armchair triangles can be used as building blocks for other types of flakes that support the ghost states. Edge roughness has only a small effect on the level structure of the triangular flakes, but the effect is considerably enhanced in the other types of flakes. In round flakes, the states near the Fermi level depend strongly on the flake radius, and they are always localized on the zigzag parts of the edge.

PACS numbers: 73.21.La, 81.01.Uw, 61.48.De

1. Introduction

Nearly free electrons trapped by a high-symmetry potential exhibit a shell structure that arises from the symmetry-induced degeneracy and bunching of energy levels of different radial modes. Such level structure has been observed in metallic clusters and semiconductor quantum dots (for reviews see [1, 2]). Usually, the shell structure is associated with a spherical or circular symmetry, but it exists also, for example, in three-dimensional icosahedral [3] and two-dimensional triangular clusters [4]. The shell structure is a single-particle property and can be understood on the basis of the jellium model of delocalized electrons [5] or the tight-binding approach [6].

In two-dimensional systems, the most interesting confinement geometries for electrons are a circle, hexagon, and triangle. Obviously, the circle has the highest symmetry of these and the triangle the lowest. Surprisingly, however, it is the triangle that has the most persistent shell structure and also a regular supershell structure [7]. The triangular shape is preferred in two-dimensional metallic systems [4, 8, 9], in plasma clusters [10], and it is observed also in semiconducting silicon clusters [11].

The shell structure of quantum dots and metal clusters is caused by nearly free conduction electrons. In the case of graphene, the situation is different due to the peculiar band structure. The Fermi surface consists of a set of discrete points, and the electron (hole) dispersion relation of the conduction (valence) band is linear. Recent experiments have shown that nanometer-sized graphene flakes can be produced on various surfaces [12, 13, 14, 15, 16, 17, 18], which has induced a significant amount of theoretical interest [19, 20, 21, 22, 23, 24, 25, 26, 27, 28, 29, 30].

In this article, we show that finite graphene flakes (or quantum dots) have an interesting energy spectrum close to the Fermi level. The most common edges of graphene are the so-called armchair and zigzag edges. It turns out that the energy spectrum of graphene flakes depends strongly on the type of the edge, and that flakes of similar size and shape can exhibit distinctly different electronic structure (selection rules). In an earlier report [31], we reported results for triangular graphene flakes and showed that a simple tight-binding (TB) model that considers only the carbon p_z electrons produces a similar shell structure than a full electronic structure calculation with all the valence electrons (based on the density functional theory, DFT). Moreover, the results showed that the electronic levels close to the Fermi energy can be understood as those of free massless electrons confined in a triangular cavity. Herein, we shall further investigate the peculiarities of the graphene electronic structure that are caused by the geometry and edge structure of the flake.

The atomic p_z electrons perpendicular to the graphene plane are responsible for the band structure shown in figure 1, where the valence and the conduction bands meet at the corners of the hexagonal Brillouin zone [32, 33]. The Fermi surface consists of a discrete set of these points of high- k value, and the resulting density of states (DOS) has a zero weight (as well as zero band gap) at the Fermi energy ϵ_F . The dispersion relation is linear in the near vicinity of the Fermi level. Since the atomic p_z electrons are perpendicular to the graphene plane their interaction with the neighboring atoms does not have any directional dependence and the TB model can be reduced to the traditional Hückel model

$$H_{ij} = \begin{cases} -t, & \text{if } i, j \text{ nearest neighbours} \\ 0, & \text{otherwise} \end{cases} \quad (1)$$

where the hopping parameter t (resonance integral) determines the width of the bands and the on-site energy is chosen to be $\epsilon_F = 0$. We present our results in units $t = 1$

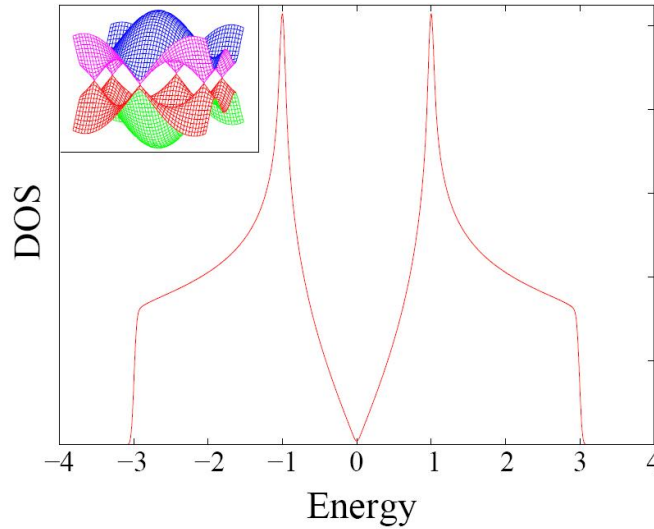


Figure 1. The density of states (p_z electrons) of an infinite graphene sheet for the TB method used. Inset: cross-over of the valence and conduction bands at the Fermi energy.

(in real graphene our unit t corresponds to about 2.6 eV). It is important to note that the simple TB model becomes equivalent to that of the free electron model when the electron wave length becomes much larger than the interatomic distance [6]. This is valid at the bottom of the valence band where the free electron model gives the correct shell and supershell structure [31]. The situation is more complicated near the Fermi level where the electron wave length ascribes to the interatomic distance. However, as we shall see, also there the level structure can be understood in terms of the free electron model, but now for *massless* electrons.

In the following, we consider graphene flakes that are cut out from a perfect infinite graphene sheet and neglect the effects of the substrate as well as the passivation of dangling bonds. The passivation, say with hydrogen, involves sp^2 hybridized orbitals and is expected to have only a marginal effect on the perpendicular p_z electron states [32, 33]. This approximation was supported by our earlier work where we compared the full DFT calculations of hydrogen passivated graphene flakes with the results of the simple Hückel model without passivation [31]. Note however, that our simple model can not account for possible spin-polarization of the edge states with large degeneracy[34].

2. Triangular graphene flakes

The Fermi level of graphene consists of two equivalent points at the border of the Brillouin zone (see figure 1) where the conduction and valence bands open as circular cones resulting in a linear dispersion relation for electrons $\epsilon(\mathbf{k}) = C\hbar k$, where C is the velocity. Thus, it is to be expected that the electron dynamics is not determined by the Schrödinger equation but by the equation of massless particles (Klein-Gordon or Dirac equation). The simple wave equation for a triangular cavity has an analytic

solution [35] which gives the energy eigenvalues

$$\epsilon_{n,m} = \epsilon_1 \sqrt{n^2 + m^2 - nm}, \quad (2)$$

where m and n are positive integers with $n \geq 2m$. The state with $n = 2m$ is nondegenerate while states with $n > 2m$ have a degeneracy 2. In our case $\epsilon_1 = 2\pi t/\sqrt{3N}$, N being the number of atoms. In the case of Schrödinger equation (i.e. electrons with mass), the exact solution gives $\epsilon \propto n^2 + m^2 - nm$, i.e. Eq. (2) without the square root. It is interesting to note that the exact solution for the wave equation was presented by Lamé already in 1852 [36], as noted by Krishnamurthy who studied the corresponding solution of the Schrödinger equation [37]. The corresponding wave functions can be found in [38].

The eigenvalues of Eq. (2) are solutions of the wave equation for massless particles, for example, for elastic waves, for electromagnetic waves or for the positive energy solutions of the Klein-Gordon equation. We want to emphasize that we have not shown that they are solutions of the Dirac equation where the boundary conditions are tricky for a cavity [21, 30, 39]. However, our numerical solutions of the TB problem for large triangular flakes are in excellent agreement with those of Eq. (2).

The electronic density of states (DOS) of a finite system (flake) consists of a set of discrete energy levels. Instead of plotting the level structure it is more useful to study the density of levels since it points out more clearly the exact and nearly exact degeneracies of levels as well as the shell structure, which manifests itself as a regular variation of the level density. It is thus useful to define a continuous DOS by using a Gaussian convolution of the discrete levels ϵ_i :

$$g(\epsilon) = \frac{1}{\sigma\sqrt{2\pi}} \sum_i e^{-(\epsilon-\epsilon_i)^2/2\sigma^2}, \quad (3)$$

where σ is the width of the Gaussian.

Figure 2 shows TB-DOS above the Fermi energy for three graphene triangles (~ 22000 , 15000 and 5600 atoms) with armchair and zigzag edges and compares them with the DOS of free massless electrons (see Eq. (2)). For armchair flakes, the comparison includes now additional (forbidden) index values $m = n$. The results are the following: (i) Each energy level has an additional degeneracy of two due to the two equivalent points at ϵ_F . (ii) The zigzag triangle shows the levels of equation (2) with index values $m \geq 1$ and $n \geq 2m$ while the armchair edge shows also those where $n = m$. We call these additional states (where $n = m$) as “ghost states”. (iii) Equation (2) describes only the lowest states accurately and is more successful for larger triangles. (iv) Due to the sparseness of the states, supershell oscillations of the massless particles become visible only in the large triangles (although they are visible at the bottom of the band already in small triangles [31]). (v) The zigzag edge supports particularly visible edge states [41, 42] that appear at ϵ_F as a prominent peak (figure 2). The number of these states equals the number of the outermost edge atoms in zigzag triangles, which is $N_{ss} = \sqrt{N}$. We shall return to the edge states in section 6.

Graphene ribbons with armchair edge show density of states with or without a gap, depending of width of the ribbon [42]. In the case of triangular flakes with armchair edge no such effect was seen. The only size dependence observed was the scaling of the energy levels with the flake size.

The lowest conduction states that are numbered in figure 2 show fascinating details, and the electron densities of such states are visualized in figure 3. The above-mentioned ghost states (left, labeled by odd indices) show an interesting feature as

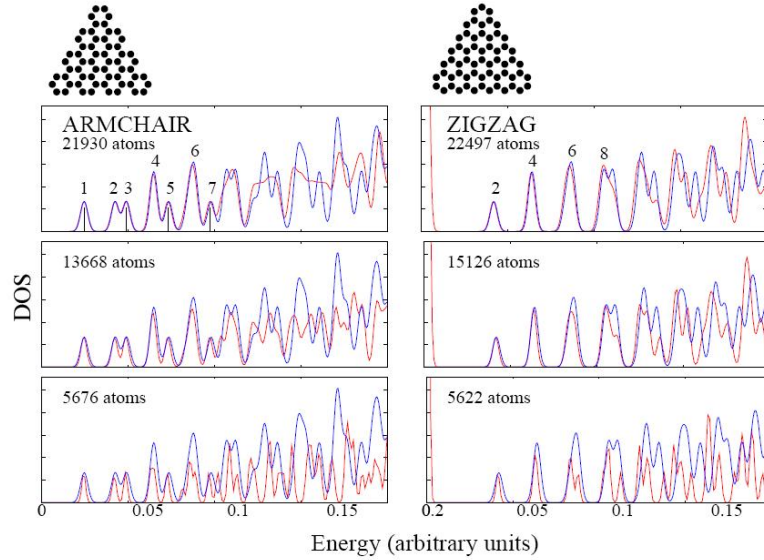


Figure 2. TB-DOS above the Fermi energy for triangular flakes (red curves), compared to the DOS of equation (2) (blue curves). The sizes of the triangles are given as numbers of atoms. Note that the triangles showing the geometries are much smaller. The energy is in units of t for the largest armchair and zigzag triangles, respectively. For the smaller sizes the energy has been scaled by the square root of the number of atoms in order to get the peaks at the same positions.

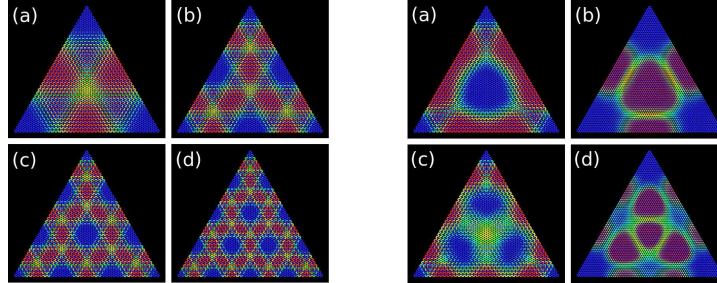


Figure 3. LEFT FOUR: Electron density of (a) the 1st, (b) 3rd, (c) 5th, and (d) 7th energy levels above the Fermi energy in armchair triangles (“ghost states”, labeled in Fig. 2). Each level has a degeneracy of two. RIGHT FOUR: Electron density of ((a) and (b)) the 2nd and ((c) and (d)) the 4th energy levels above the Fermi energy (labeled in Fig. 2) for armchair and zigzag triangles of 4920 and 5181 C atoms, respectively. Color scale from blue to red, blue corresponds to vanishing density. Each figure shows the sum of the densities of the degenerate states.

they have a simple geometric pattern of triangular symmetry. The size (number) of the triangles decreases (increases) with increasing energy, i.e. the pattern repeats itself. These ghost states are completely absent for the zigzag triangles, and they correspond to quantum numbers of Eq. (2) not allowed for free electrons in a triangular box (i.e. $n = m$ (with extra degeneracy) in Eq. (2)). Previously, we calculated the same states for a smaller armchair triangle with a DFT method (330 C atoms, 60 passivating H

atoms) [31]. The internal structure (symmetry) of the states was clearly similar, and therefore, the phenomenon is independent of the triangle size and the model used. We shall discuss the ghost states in detail in Section 4.

Figure 3 (right) shows the electron densities corresponding to the “normal” low energy states that obey the standard selection rules ($m \geq 1$ and $n \geq 2m$). Again, the electron density does not necessarily vanish at the edges of the triangle. Interestingly, the corresponding states for the armchair and zigzag triangles (with the same energy and quantum numbers n and m) display nearly an anticorrelation: The maxima in zigzag triangles are minima in armchair triangles and vice versa. Overall, the states close to the Fermi level appear very different from those at the bottom of the band. They are *not* simple densities of massless particles confined in a triangular cavity since the density profile does not decay to zero at the edges. The corresponding electron levels are close to the Brillouin zone boundary, having large k -values, and the wave functions have pronounced oscillations with wave lengths that are related to the hexagonal unit cell size. These oscillations enable that the wave function can be formally zero at the edges, but the corresponding pseudowave function of the massless particle does not necessarily vanish.

3. Hexagonal graphene flakes

Similar TB calculations were performed for hexagonal graphene flakes with armchair and zigzag edges. The comparison between hexagonal and triangular flakes is based on hexagons that were cut from the corresponding triangles (taking the corners off). In general, the level structure is more complicated but some similarities with the triangular flakes can be found. We observe the following results: (i) The zigzag edge supports edge states (see section 6) while the armchair edge results in a gap at ϵ_F . (ii) The electron densities of the states *near* ϵ_F display the main amplitude at the edges/corners both for the zigzag and armchair edges. (iii) For the zigzag flake, the number of states near the Fermi level depends on the size of the flake. (iv) Hexagonal flakes display few states that have exactly the same electron density as the original triangles (cutting off the corners). (v) In most cases, the electron densities are different than in the corresponding triangular flakes or hexagons with the other type of edge. It is also worth mentioning that at the bottom of the valence band the (p_z) electrons act as free particles not seeing the atomic lattice, which is a case similar to triangles. This makes the supershell structure visible at the bottom of the valence band, but it is not as clear as in the triangular graphene flakes.

Figure 4 shows the DOS of hexagonal flakes. In the armchair panel (right), the DOS has been scaled by size in order to get the peaks to coincide near the Fermi level. The scaling factor $\sqrt{N_1/N_2}$ is the same as in the case of triangles. In the zigzag flakes, the scaling does *not* bring the peaks at the same positions. This is a special feature that does not exist in triangular flakes. In general, the zigzag flakes have a peak and the armchair flakes display a gap at ϵ_F , which is the case for triangles also. The hexagonal armchair flakes display states near the Fermi level that are in a sense universal: they do not depend on the size of the flake (cf. triangles, figure 2). The armchair flakes do not exhibit any states that could be regarded as ghost states suggesting that these are characteristic for the armchair triangles only. However, as will be shown in Section 4, a slight modification of the hexagonal flakes changes the situation. We also note that the DOS near the Fermi energy has some peaks that coincide with the ones of the triangles, and there is one state that is common in all

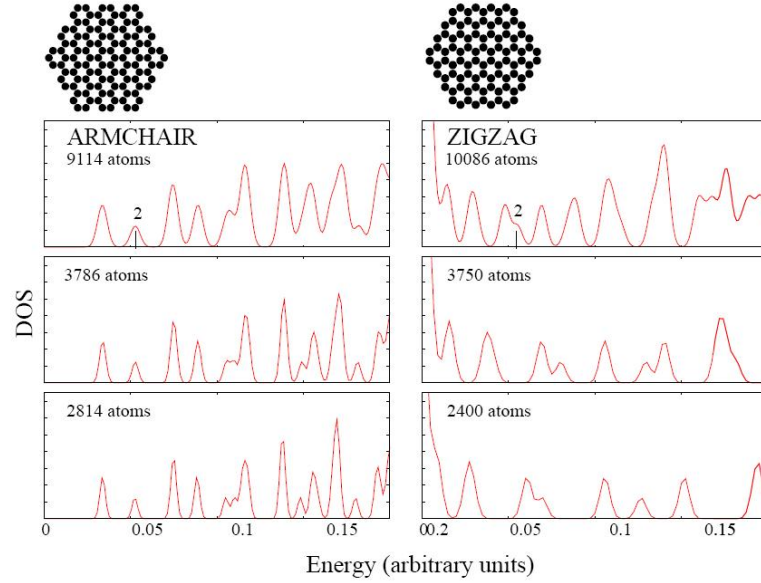


Figure 4. TB-DOS of the hexagonal flakes with armchair (left panel) and zigzag (right panel) edge. The energy is in units of t for the largest hexagons. For the smaller sizes the energy has been scaled by the square root of the number of atoms (scaling factor = $\sqrt{N_1/N_2}$, where N_1 is the number of atoms in the flake 1 and N_2 atoms in the flake 2). The geometries are shown as small hexagons.

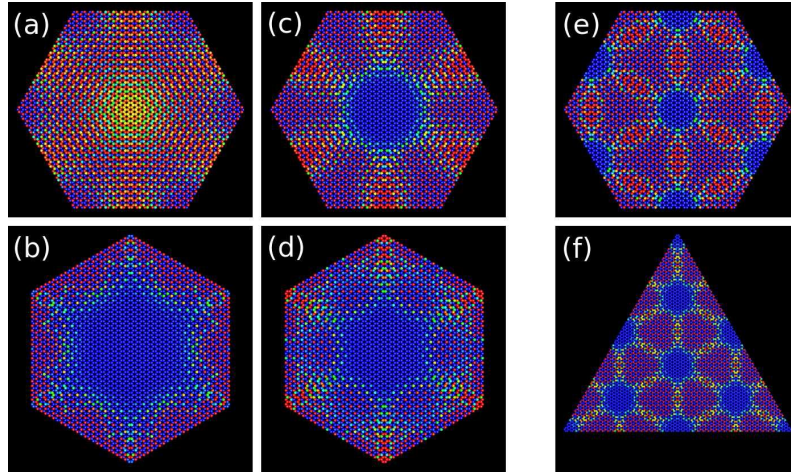


Figure 5. Electron density corresponding ((a) and (b) the first peak before the peak “2” in Fig. 4) and ((c) and (d) the peak “2” for the armchair (upper) and zigzag (lower) hexagons. (e) and (f) show a state that occurs both in the armchair-edged hexagon and triangle (peak “6” in Fig. 2). Color scale from blue to red, blue corresponds to vanishing density.

the triangular and hexagonal flakes: the peak “2” in figures 2 and 4. Furthermore, the states that have exactly the same energies in armchair triangles and hexagons display

similar electron densities due to the common symmetry properties (figure 5(e) and (f)).

4. Ghost states

The hexagonal armchair flakes of section 3 do not exhibit the peculiar ghost states. The reason is that our flakes obey the armchair construction exactly: the corners are those of a perfect honeycomb pattern. However, the ghost states will re-appear if the flakes are built differently. This can be understood by studying a triangular armchair flake with ghost states (figures 6(a)-(b)). The boundary conditions of the tight-binding problem require that the wave function is zero at the (imaginary) lattice sites just outside the triangle. Now, we can put two triangles together as in the rhombus-shaped flake shown in Fig. 6(c), and add an additional row of atoms between the triangles. This system has naturally the same ghost states as the original triangle. Similarly, we can construct hexagonal flakes with ghost states as shown in Fig. 6(d), and it is clear that any shape consisting of equilateral triangles can exhibit ghost states. The only requirement is that an additional row of lattice sites (atoms) is added at the interface of the triangles. The ghost states in different triangles are then completely decoupled although they appear as continuous wave functions, and the wave function is exactly zero at the interface. This is also the reason why the ghost state pattern repeats itself: The high-index (large $n = m$) ghost states are the same in large triangles as the low-index ghost states in small triangles, and the energy is exactly the same if the side length L of the large triangle is commensurate with that of the small triangle.

At this point, it is important to note that the hexagonal flakes constructed according to the prescription above do not have perfect corners. Instead of the armchair edge just bending over, they have a small region of zigzag edge at the corners. Similarly, the extra row of atoms in the rhombus shown in figure 6 results in that the corners do not follow the armchair construction. The ghost states disappear, if the rhombus is made by merging two triangles together without an additional row of atoms.

The appearance of ghost states in the TB model reflects the balance between the graphene band structure and the free electron states in two-dimensional systems. Figure 6 (e) shows the combined density of two degenerate plane waves for free electrons, which can be expressed as

$$n(x, y) = \sin^2 qx + \sin^2\left(\frac{1}{2}qx + \sqrt{3}qy\right) + \sin^2\left(\frac{1}{2}qx - \sqrt{3}qy\right). \quad (4)$$

This density has a clear similarity of that of the ghost states, except that the rapid oscillations from atom to atom are absent. Again, we want to remind that the (pseudo) wave function of these ‘‘Dirac fermions’’ above the Fermi energy does not need to be zero at the edge of the triangular cavity since the rapid oscillations take care of this boundary condition. Thus, also solutions where the derivative of the pseudowave function is zero are allowed.

5. Edge roughness

The effect of edge roughness was studied for triangular and hexagonal flakes. We removed randomly 10, 38, or 50 percent of edge atoms and studied how it affected the DOS and electron densities of the states near ϵ_F . The atom removal process avoided

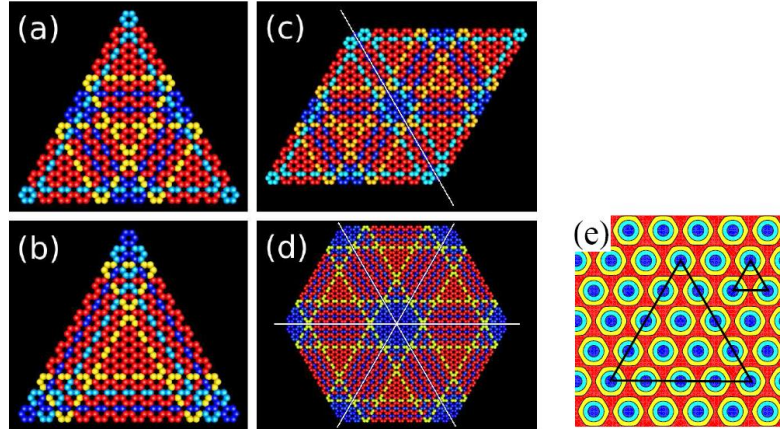


Figure 6. Ghost states in ((a) and (b)) armchair triangles, and the corresponding ghost states (2nd and 1st) in (c) an imperfectly built rhombus and (d) hexagon. The extra rows of atoms are marked with the narrow white lines. (e) shows a standing wave solution of the wave equation in an infinite two-dimensional (hexagonal) system. The small and large triangles in (e) demonstrate how the ghost states (1st and 4th) appear in triangular flakes.

situations where the possible remaining atom had only one nearest-neighbour, and such atoms were taken out.

The results are collected in figure 7 which shows the TB-DOS above the Fermi energy (upper panel) and the electron density of the 2nd conduction electron state (peak “2”, lower panel). Especially in the case of hexagonal flakes, the edge roughness has a noticeable effect on DOS and electron densities. Already a small edge roughness causes the degeneracy of the states to break up, and for example, removal of only 10% of edge atoms in the zigzag-edged hexagonal flake results in a significant perturbation, and the electron density pattern of the intact flake cannot be identified anymore. The changes are less dramatic for triangular flakes, and the pattern of the 2nd conduction state is always recognizable. The DOS curves indicate that the states closest to ϵ_F are the most robust against edge roughness. Finally, the electron density of the corresponding states seems to avoid the rough parts of the edge in the case of armchair edge and favor them in the case of zigzag edge.

6. Round graphene flakes

Finally, we have studied round (circular) graphene flakes. Round flakes were cut out of a graphene sheet as follows: The center was chosen to be a high-symmetry point (an atom or a center of a hexagon), and all the atoms inside a chosen radius were included. After this, all the edge atoms with only one nearest-neighbour were removed. The number of atoms is thus determined by the chosen radius and center. Figure 8 shows the TB-DOS above the Fermi level for four round graphene flakes with almost the same diameter and ~ 5000 atoms. Based on the triangular and hexagonal graphene flakes, one might expect that the shell structure is independent of the size. Figure 8 demonstrates that this is clearly not the case. On the contrary, the level structure is very sensitive to the flake diameter. This can be understood by inspecting

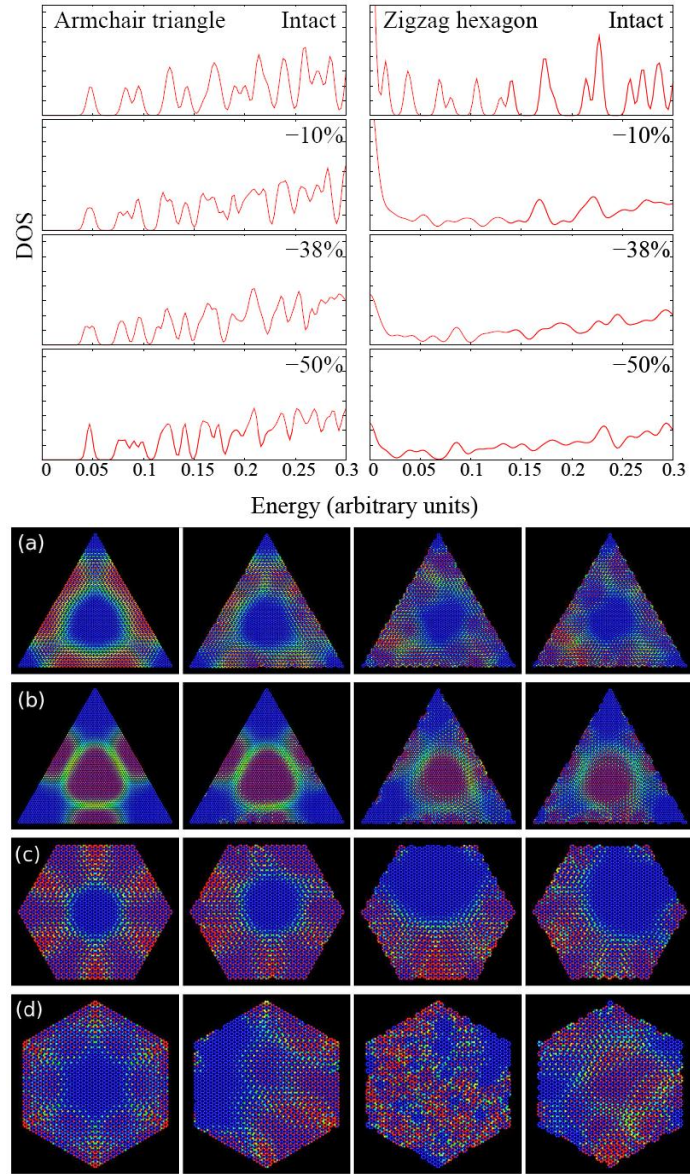


Figure 7. UPPER PANELS: Effect of the edge roughness on TB-DOS for an armchair triangle (left) and zigzag hexagon (right). LOWER PANELS: Effect of the edge roughness on the electron density of the 2nd conduction electron state for armchair and zigzag flakes. Triangular flake with (a) armchair edge and (b) zigzag edge. Hexagonal flake with (c) armchair edge and (d) zigzag edge. From left to right: Intact edge, 10, 38, and 50 percent of the edge atoms removed. Color scale from blue to red, blue corresponds to vanishing density.

the structure of the low-energy wave functions (lower panel in figure 8). The states above the Fermi energy are localized close to the flake edges, and therefore, they experience the detailed edge geometry.

The edge of a circular flake comprises not only the simple armchair and zigzag segments, but also more complicated parts. Figure 8 shows the electron density of the lowest state above the Fermi level. In all cases, the electron density is concentrated in the zigzag regions. The length and distribution of the zigzag segments varies with the flake diameter (size). This causes that the energy of the corresponding state is different for each round flake. The same argument applies for all the low-energy states since they have marked amplitudes at the edges, and it explains the strong size-dependence of DOS. The edge states have large degeneracy (or near degeneracy) as seen as a large peak at zero energy in the plots of the density of states in Figs. 2, 4, and 8b. This can cause spin-polarization in a partially filled case due to the Hund's first rule, but this is out of the reach of our simple model.

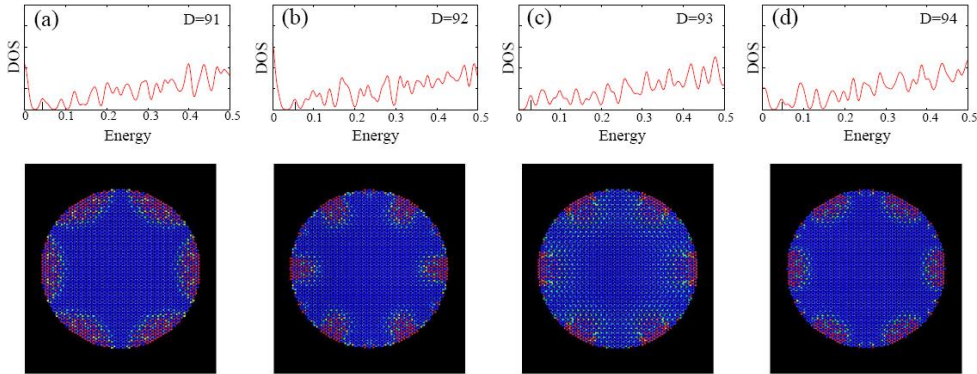


Figure 8. TB-DOS of round graphene flakes (upper panel) and electron densities (lower panel) of the first conduction electron state above ϵ_F (marked with a tic in the DOS panels). The flake diameters (D) are (left to right): 91, 92, 93, and 94 times the nearest-neighbour distance corresponding to 4980, 5118, 5238, and 5338 atoms, respectively. Color scale from blue to red, blue corresponds to vanishing density.

The edge states are visible in the zigzag triangles and hexagons, and they appear as a prominent peak (DOS) at the Fermi energy. For triangles, all the edge states have zero energy, i.e. they are exactly at the Fermi level. The hexagon edge states are also concentrated at the Fermi energy, but they have a small dispersion. The situation is significantly different in round flakes due to the fact that the lengths of the zigzag regions are very small. This leads to a situation where the electrons become localized and their energy increases. Figure 9 shows the total electron density of edge states in these three cases: In the case of triangles, the edge states bend smoothly around the corners of the triangle, but for hexagons they are already pushed out from the corners. The round flakes exhibit edge states that are localized in narrow regions and penetrate much deeper inside the flake.

7. Conclusions

We have computed the electronic structure of triangular, hexagonal and round graphene flakes by using a TB method that considers the carbon p_z electrons. We observe that the DOS close to the Fermi energy ϵ_F is independent of the size of the

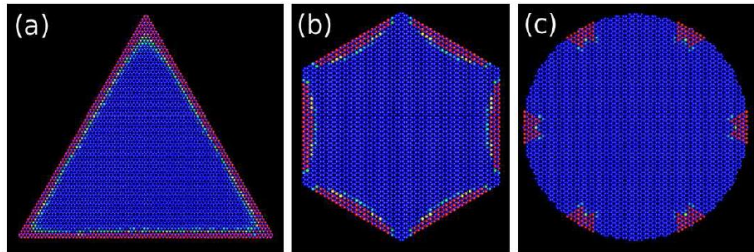


Figure 9. Electron density of the edge states (DOS peak at ϵ_F) for (a) a zigzag triangle (5622 atoms, 72 states), (b) zigzag hexagon (3750 atoms, 18 states), and (c) round flake (5118 atoms, 12 states). Color scale from blue to red, blue corresponds to vanishing density.

triangles and armchair-edged hexagons, but depends strongly on the size of the zigzag hexagons and round flakes. The triangles with zigzag edge exhibit the well-known edge states, while the armchair triangles show an additional set of “ghost states” which result in from the interplay between the graphene band structure and the plane wave solutions of the wave equation. The same ghost states will emerge in any flake of graphene that can be constructed from equilateral armchair triangles of the same size with additional rows of atoms in the boundaries.

Also hexagons can be constructed with armchair or zigzag edges. In the case of the armchair edge, the shell structure is clear and scalable with the flake size (cf. triangles). However, for the zigzag edge the shell structure of the hexagonal confinement is disturbed by the edge states, and the level structure above the Fermi energy depends on the size of the hexagon.

For round graphene dots, one might expect the shell structure of a circular cavity. However, the low-energy level structure (above ϵ_F) is dominated by the edge states that appear in the zigzag regions of the edge, and the lengths and distribution of such segments vary with the flake diameter. Consequently, the level structure is very sensitive to the size of the circular graphene flake.

The effect of the edge roughness on shell structure was studied by removing a fraction of atoms randomly. In the armchair triangles, the shell structure is simple and scalable, and the roughness has only a small effect on the low energy states. For the zigzag hexagons, the low-energy levels are edge-related, and already a small roughness removes the shell structure.

We have obtained our results for free graphene flakes and not considered the interaction with substrate or electric leads which evidently could have effects of the shell structure. However, transport spectroscopy through semiconductor quantum dots[43] have shown that the shell structure calculated for free dots[44] can indeed be captured with weak connections to leads. A more direct measurement of the electronic states would be scanning tunneling microscopy which has already been used to study suspended graphene[45]. It is possible that on a proper surface STM spectroscopy could reveal the detailed structures of the electron wave functions.

References

- [1] de Heer WA, (1993) *Rev. Mod. Phys.* **64** 677
- [2] Reimann SM and Manninen M, (2002) *Rev. Mod. Phys.* **74**, 1283

- [3] Mansikka-aho J, Hammarén E, and Manninen M, (1992) *Phys. Rev. B* **46**, 12649.
- [4] Reimann S M, Koskinen M, Häkkinen H, Lindelof P E and Manninen M 1997 *Phys. Rev. B* **56** 12147.
- [5] Ekardt W, (1984) *Phys. Rev. Lett.* **52** 1925.
- [6] Manninen M, Mansikka-aho J and Hammarén E 1991 *Europhys. Lett.* **15** 423.
- [7] Brack M, Blaschke J, Greagh S C, Magner A G, Meier P and Reimann S M 1997 *Z. Phys. D* **40** 276.
- [8] Kolehmainen J, Häkkinen H, and Manninen M 1997 *Z. Phys. D* **40** 306.
- [9] Janssens E, Tanaka H, Neukermans S, Silverans R E and Lievens P 2003 *New J. Phys.* **5** 46.
- [10] Reimann S M, Koskinen M, Helgesson J, Lindelof P E and Manninen M 1998 *Phys. Rev. B* **58** 8111.
- [11] Lai M Y and Wang Y L 1998 *Phys. Rev. Lett.* **81** 164.
- [12] Berger C, Song Z M, Li T B, Li X B, Ogbazghi A Y, Feng R, Dai Z T, Marchenkov A N, Conrad E H, First P N and De Heer W A 2004 *J. Phys. Chem.* **108** 19912.
- [13] Novoselov K S, Geim A K, Morozov S V, Jiang D, Zhang Y, Dubonos S V, Grigorieva I V and Firsov A A 2004 *Science* **306** 666.
- [14] Novoselov K S, Geim A K, Morozov S V, Jiang D, Katsnelson M I, Grigorieva I V, Dubonos S V and Firsov A A 2005 *Nature* **438** 197.
- [15] Berger C, Song Z M, Li X B, Wu X S, Brown N, Naud C, Mayo D, Li T B, Hass J, Marchenkov A N, Conrad E H, First P N and De Heer W A 2006 *Science* **312** 1191.
- [16] Novoselov K S, Jiang Z, Zhang Y, Morozov S V, Stormer H L, Zeitler U, Maan J C, Boebinger G S, Kim P and Geim A K 2007 *Science* **315** 1379.
- [17] Geim A K and Novoselov K S 2007 *Nature materials* **6** 183.
- [18] Li G and Andrei E A 2007 *Nature Phys.* **3** 623.
- [19] Alicea J and Fisher M P A 2005 *Phys. Rev. B* **74** 75422.
- [20] Gusynin V P and Sharapov S G 2005 *Phys. Rev. Lett.* **95** 146801.
- [21] Tworzydło J, Trauzettel B, Titov M, Rycerz A, Beenakker C W J, *Phys. Rev. Lett.* **96**, 246802 (2006).
- [22] Gusynin V P, Sharapov S G and Carbotte J P 2006 *Phys. Rev. Lett.* **96** 256802.
- [23] Zhou S Y, Gweon G H, Graf J, Fedorov A V, Spataru C D, Diehl R D, Kopelevich Y, Lee D H, Louie S G and Lanzara A 2006 *Nature Phys.* **2** 595.
- [24] Yamamoto T, Noguchi T and Watanabe K 2006 *Phys. Rev. B* **74** 121409.
- [25] Nomura K and MacDonald A H 2007 *Phys. Rev. Lett.* **98** 76602.
- [26] Son Y W, Cohen M L and Louie S G 2007 *Phys. Rev. Lett.* **97** 216803.
- [27] Areshkin D A, Gunlycke D and White C T 2007 *Nano Lett.* **7** 204.
- [28] Chen J-H, Jang C, Xiao S, Ishigami M and Fuhrer M S, *Nature Nanotech* **3**, 206 (2008).
- [29] Castro E V, Peres N M R, Lobos dos Santos JMB, Castro Neto A H and Guinea F, *Phys. Rev. Lett.* **100**, 026802 (2008).
- [30] Akhmerov A R and Beenakker C W J, *Phys. Rev. B* **77**, 085423 (2008).
- [31] Akola J, Heiskanen H P and Manninen M, 2008 *Phys. Rev. B* **77** 193410.
- [32] Wallace P R, *Phys. Rev.* **71**, 622 (1947).
- [33] Elliot S R 1998 *The Physics and Chemistry of Solids* (John Wiley & Sons, New York).
- [34] Son Y-W, Cohen M L and Louie S G, *Nature* **444**, 347 (2006).
- [35] Borghis F E and Papas C H 1957 *Encyclopedia of Physics* (Flückel S, Springer, Berlin).
- [36] Lamé M G, *Leçons sur le Théorie Mathématique d'Elasticité des Cores Solides* (Bachelier, Paris 1852).
- [37] Krishnamurthy H R, Mani H S and Verma H C 1982 *J. Phys. A: Math. Gen.* **15** 2131.
- [38] Doncheski M A, Hepplemann S, Robinet R W, and Tussey D C, *Am. J. Phys.* **71**, 541 (2003).
- [39] Castro Neto A H, Guinea F, Peres N M R, Novoselov K S and Geim A K, arXiv:0709.1163v2.
- [40] Huang Y -Z, Guo W -H, Yu L -J, and Lei H -B 2001 *IEEE J. Quantum Electrodynamics* **37** 1259.
- [41] Kobayashi K 1993 *Phys. Rev. B* **48** 1757.
- [42] Nakada K, Fujita M, Dresselhaus G and Dresselhaus M S 1996 *Phys. Rev. B* **54** 17954.
- [43] Tarucha S D, Austing G, Honda, van der Haage R J, and Kouwenhoven L, *Phys. Rev. Lett.* **77**, 3613 (1996).
- [44] Koskinen M, Manninen M and Reimann S M, *Phys. Rev. Lett.* **79**, 1389 (1997).
- [45] Li G, Luican A, and Andrei E Y, arXiv:0803.4016v1.